Stability and Power Characteristics of a Simplified Model of Boost Converter with Photovoltaic Input

Maho Wakabayashi, Toshiyasu Ohata and Toshimichi Saito
Department of Electrical and Electronics Engineering, HOSEI University
Koganei-shi, Tokyo, 184-8584 Japan, tsaito@hosei.ac.jp

***Abstract*— This paper studies a simple switched dynamical system based on the boost converter with photovoltaic input. Applying a simple piecewise linear modeling and mapping procedure that system dynamics can be analyzed precisely. We have analyzed stability of fundamental periodic phenomena and their power characteristics. Especially, we have clarified that unstable periodic orbit can have larger average power than stable periodic orbit.**

I. Introduction

The switched dynamical system (SDS [1]-[3]) consists of continuous subsystems connected by a discrete switching rule. Depending on the rule and parameters, the SDSs can exhibit various periodic/chaotic phenomena and related bifurcation phenomena. As typical and concrete examples of the SDSs in engineering systems, switching power converters and A/D converters have been studied.

This paper studies stability and basic bifurcation phenomena of a simple SDS based on the boost converter with photovoltaic (PV) input. Power converters of the PV input has been attracted a lot of attention as efficient renewable energy systems [4]-[6]. In our system, the PV input corresponds to a solar cell. The PV input is applied to the dc-dc boost converter with current mode control switching.

In order to simplify the analysis, we replace the smooth voltage-current characteristics of the PV with two-segment piecewise linear characteristics [7] [8]. Also, assuming a high frequency operation, we replace the output load with a constant voltage source [9]. Deriving one-dimensional return map of a state variable at every switching instants, we can analyze stability of fundamental periodic waveforms and their power characteristics precisely. Especially, we have clarified that unstable periodic orbit can have larger average power than stable periodic orbit. Basic bifurcation phenomena have also been considered. Now we are trying to fabricate a simple test circuit and to confirm typical phenomena experimentally.

II. Circuit and State Equation

Figure. 1 shows the simplified model of the boost converter with photovoltaic inputs. Here we derive a dimensionless state equation of the simple SDS based on the boost converter with PV input. First, we simplify the PV input by 2-segment piecewise linear current-controlled voltage source (CCVS):

$$V_i(i) = \begin{cases} -\gamma_a(i - I_P) + V_P & \text{for } i \le I_P \\ -\gamma_b(i - I_P) + V_P & \text{for } i > I_P \end{cases} \quad (1)$$

The boost converter has a switch S and a diode D. They can be either of the following 2 states:

State 1: S conducting and D blocking
State 2: S blocking and D conducting.

The switching rule is defined by

$$\begin{array}{l} \text{State 1} \rightarrow \text{State 2 at } t = nT \text{ and } i > J_- \\ \text{State 2} \rightarrow \text{State 1 when } i = J_- \end{array} \quad (2)$$

where J_- is the lower threshold. Figure 2 illustrates the switching rule. Let the system be State 1. If a clock pulse arrives at time $t = nt$ then State 1 is switched into State 2. If an inductor current i reaches the lower threshold then State 2 is switched into State 1. Repeating such operations, the system can exhibit a variety of periodic /chaotic phenomena. Assuming that time constant is much larger than the clock

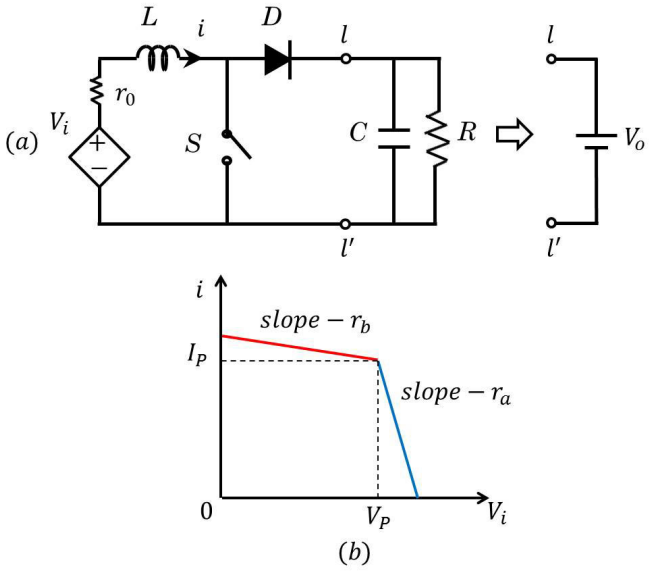

Fig. 1. The boost converter with photovoltaic inputs and simplification

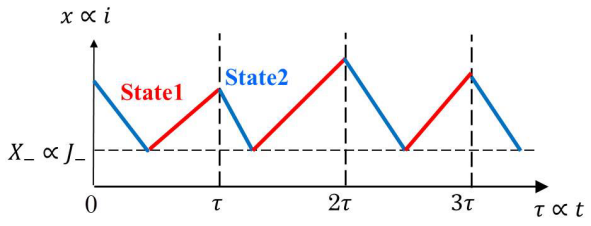

Fig. 2. Switching rule

period T, we can simplify the output load into a constant-voltage source V_o. The circuit dynamics is described by

$$L\frac{di}{dt} = \begin{cases} V_i(i) & \text{for State 1} \\ V_i(i) - V_0 & \text{for State 2} \end{cases} \tag{3}$$

Using the following dimensionless variables and parameters,

$$\tau = \frac{t}{T},\ x = \frac{i}{I_P},\ y(x) = \frac{T}{LI_P}V_i(I_P x),\ \alpha = \frac{\gamma_a I_P}{V_P}$$
$$\beta = \frac{\gamma_b I_P}{V_P}, q = \frac{V_o}{V_P},\ \gamma = \frac{TV_P}{LI_P},\ X_- = \frac{J_-}{I_P}, \tag{4}$$

Eqs. (1) and (3) are transformed into

$$\frac{dx}{d\tau} = \begin{cases} \gamma y(x) & \text{for State 1} \\ \gamma(y(x) - q) & \text{for State 2} \end{cases} \tag{5}$$

$$y(x) = \begin{cases} -\alpha(x-1)+1 & \text{for } x \le 1 \\ -\beta(x-1)+1 & \text{for } x > 1 \end{cases} \tag{6}$$

SW Rule:

$$\begin{aligned} &\text{State 1} \rightarrow \text{State 2: at } \tau = n \text{ and } x > X_- \\ &\text{State 2} \rightarrow \text{State 1: when } x = X_- \end{aligned} \tag{7}$$

The dimensionless 5 parameters can be classified into two categories: (α, β, q), which characterizes "solar cell and load", and (γ, X_-), which characterizes "switching control". γ is parameter which relates temperature. The exact piece-wise solution is given by

State 1:

$$\begin{cases} x(\tau) = (x_0 - x_{e1})e^{-\gamma\alpha(\tau-\tau_0)} + x_{e1} & \text{for } x \le 1 \\ x(\tau) = (x_0 - x_{e2})e^{-\gamma\beta(\tau-\tau_0)} + x_{e2} & \text{for } x > 1 \end{cases} \tag{8}$$

State 2:

$$\begin{cases} x(\tau) = (x_0 - x_{e3})e^{-\gamma\alpha(\tau-\tau_0)} + x_{e3} & \text{for } x \le 1 \\ x(\tau) = (x_0 - x_{e4})e^{-\gamma\beta(\tau-\tau_0)} + x_{e4} & \text{for } x > 1 \end{cases} \tag{9}$$

$$x_{e1} = 1 + 1/\alpha,\ x_{e2} = 1 + 1/\beta$$
$$x_{e3} = q/\alpha - 1 - 1/\alpha,\ x_{e4} = q/\beta - 1 - 1/\beta$$

where (τ_0, x_0) indicates an initial condition, Using these equations, we can calculate waveform precisely. In this paper we select $gamma$ as a control parameter. This parameter can represent influence of tempereture. The other parameters are fixed:

$$\alpha = 0.5,\ \beta = 5,\ q = 1.6,\ X_- = 0.7.$$

Figure 3(a) shows stable periodic orbit (PEO) with period 1. As γ decreases, it becomes unstable (Fig. 3(b)) and stable periodic orbit with period 2 appears (Fig. 3(b'))

In order to consider the power characteristics, we define the dimensionless and average powers;

$$P_A = \frac{1}{N_P}\int_0^{N_P} P_i(\tau)\,d\tau,\ P_i(\tau) = x(\tau)y(\tau), \tag{10}$$

Figure. 4 shows the instantaneous and average powers corresponding to Fig. 4. it should be noted that the average power of unstable PEO (Fig. 4 (b)) is larger than that of stable PEOs in Figs. 4 (b') and (b).

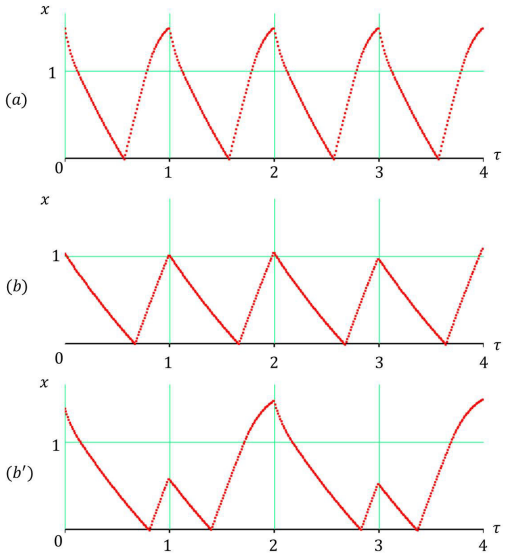

Fig. 3. Typical wavforms. (a) Stable PEO with period 1 for $\gamma \doteq 1.3$, (b) Unstable PEO with period 1 for $\gamma \doteq 0.884$. (b') Stable PEO with period 2 for $\gamma \doteq 0.884$.

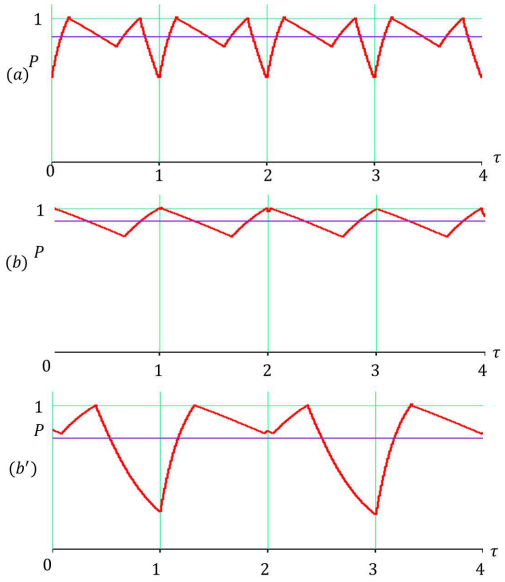

Fig. 4. Instantaneous power and average power P_a. (a) Stable PEO with period 1 fo $\gamma \doteq 1.3$, $P_a \doteq 0.87$. (b) Unstable PEO with period 1 for $\gamma \doteq 0.884$, $P_a \doteq 0.91$. (b') Stable PEO with period 2 for $\gamma \doteq 0.884$, $P_a \doteq 0.77$.

III. Return map and stability

In order to analyze the stability and power characteristics, we define the return map. Let x_n be the dimensionless current when the n-th clock arrives and the SDS is State 2 where x decreases. Since x_{n+1} is determined by x_n as shown in Fig. 5, we can define a return map $x_{n+1} = F(x_n)$. The return map can be described exactly using the exact piecewise solutions. Figure 6 shows examples of the return map corresponding to Fig. 3. The return map in Fig. 6 (a) has a stable fixed point that corresponds to stable PEO in Fig. 3 (a). Fig.6(a) shows an example of return map with stable fixed point corresponding to Fig.3(a). As $gamma$ decreases, this fixed point becomes unstable via the period doubling bifurcation and return map has stable PEO with period 2 as shown in Fig. 6 (b). The unstable fixed point and stable PEO with period 2 is corresponding to waveforms in Fig. 3 (b) and (b'), respectively.

Figure. 7 shows one-parameter bifurcation diagram for γ. We can see that, as γ decrease, the stable fixed point changed into PEO with period 2 and then to chaotic orbit.

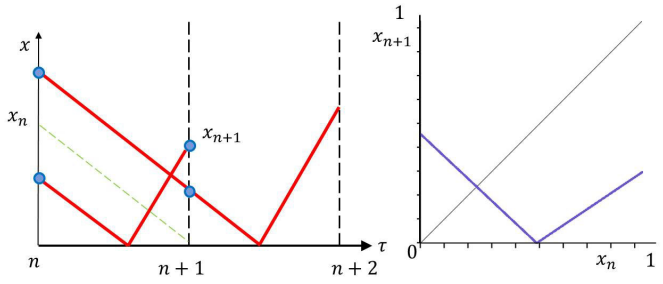

Fig. 5. Definition of return map

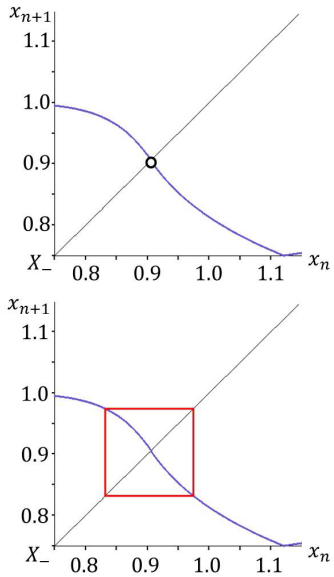

Fig. 6. Examples of the return map. (a) $\gamma \doteq 0.884$ (b) $\gamma \doteq 1.3$.

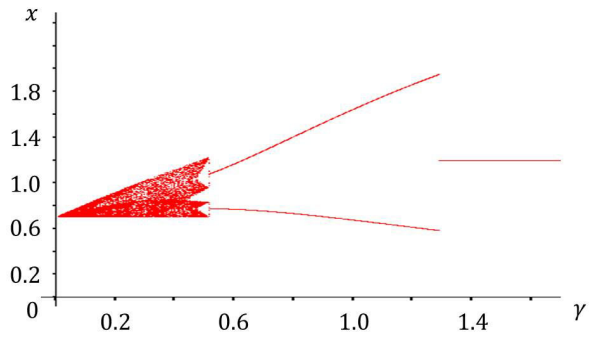

Fig. 7. Bifurcation diagram

IV. Conclusions

This paper studies a simple SDS based on the boost converter with photovoltaic input. Applying the piecewise linear simplification and mapping procedure, stability and power characteristics have been analyzed precisely. Especially, we have clarified that unstable periodic orbit can have larger average power than stable periodic orbit. Future problems include fabrication of a simple test circuit, laboratory experiments, and analysis of bifurcation phenomena.

References

[1] S. Banerjee and G. C. Verghese, eds., Nonlinear Phenomena in Power Electronics: Attractors, Bifurcations, Chaos, and Nonlinear Control, IEEE Press, 2001.

[2] C. K. Tse and M. di Bernardo, Complex behavior in switching power converters, Proc. IEEE, 90, pp. 768-781, 2002.

[3] J. H. B. Deane, P. Ashwin, D. C. Hamill and D. J. Jeffries, Calculation of the periodic spectral components in a chaotic dc-dc converter, IEEE Trans. Circuits Syst. I, 46, 11, pp. 1313–1319, 1999.

[4] H. S.-H. Chung, K. K. Tse, S. Y. Ron Hui, C. M. Mok and M. T. Ho, A Novel Maximum Power Point Tracking Technique for Solar Panels Using a SEPIC or Cuk Converter, IEEE Trans. Power Electron., 18, 3, pp. 717-724, 2003.

[5] N. D. Benavides and P. L. Chapman, Modeling the Effect of Voltage Ripple on the Power Output of Photovoltaic Modules. IEEE Trans. Ind. Electron., 55, 7, pp. 2638-2643, 2008.

[6] D. Sera, R. Teodorescu, J. Hantschel and M. Knoll, Optimized Maximum Power Point Tracker for Fast-Changing Environmental Conditions, IEEE Trans. Ind. Electron., 55, 7, pp. 2629-2637, 2008.

[7] D. Kimura and T. Saito, A Simple Switched Dynamical System based on Photovoltaic Systems, Proc. of NOLTA, pp. 487-490, 2009.

[8] H. Matsushita and T. Saito, Application of Particle Swarm Optimization to Parameter Search in Dynamical Systems, NOLTA, IEICE, E94-N, 10, pp. 458-471, 2011.

[9] T. Saito, T. Kabe, Y. Ishikawa, Y. Matsuoka and H. Torikai, Piecewise constant switched dynamical systems in power electronics, Int'l J. of Bifurcation and Chaos, 17, 10, pp. 3373-3386, 2007.